LOOK ACADEMIC PUBLISHERS
OPEN ACCESS

INTERNATIONAL JOURNAL OF ENVIRONMENTAL & SCIENCE EDUCATION
2016, VOL. 11, NO. 16, 9026-9038

Numerical Simulations of Shock Wave Refraction at Inclined Gas Contact Discontinuity

Pavel V. Bulat[a,b] and Konstantin N. Volkov[c]

[a]National Research University of Information Technologies, Saint Petersburg, RUSSIA;
[b]Mechanics and Optics University ITMO, Saint Petersburg, RUSSIA;
[c]Kingston University, London, UNITED KINGDOM

ABSTRACT

When a shock wave interacts with a contact discontinuity, there may appear a reflected rarefaction wave, a deflected contact discontinuity and a refracted supersonic shock. The numerical simulation of shock wave refraction at a plane contact discontinuity separating gases with different densities is performed. Euler equations describing inviscid compressible flow were discretized using the finite volume method on unstructured meshes and WENO schemes. Time integration was performed using a third-order Runge-Kutta method. The wave structure resulting from regular shock refraction is determined allowing its properties to be explored. In order to visualize and interpret the results of numerical calculations, a procedure for identifying and classifying gas-dynamic discontinuities was applied. The procedure employed dynamic consistency conditions and digital image processing methods to determine flow structure and its quantitative characteristics. The results of the numerical and experimental visualizations were compared (shadow patterns, schlieren images, interferograms). The results computed are in an agreement with the theoretical and experimental predictions of a regular refraction of a shock wave on an inclined contact discontinuity.

KEYWORDS
Shock wave refraction, computational dynamics, finite volume method, unstructured mesh, contact discontinuity, level-set method

ARTICLE HISTORY
Received 03 March 2016
Revised 12 April 2016
Accepted 19 May 2016

Introduction

A shock wave process (SWP) is a process of reorganizing a gas-dynamic system with the parameters f into a system with the parameters $\hat{f}$, where f and $\hat{f}$ are a set of gas-dynamic variables before and behind SWP. These sets include kinematic, thermodynamic and thermo-physical variables that define flow parameters. Specifically, examples of the variables include kinematic

CORRESPONDENCE Pavel V. Bulat ✉ pavelbulat@mail.ru

parameters (velocity, acceleration), thermodynamic parameters (pressure, density, temperature, entropy, enthalpy), and thermo-physical parameters (heat capacity, adiabatic index, viscosity), which can change during SWP.

The intensity of SWP is generally characterized by a ratio of static pressures $J = p_1/p$ behind and before SWP (p_1 is the static pressure behind SWP, and p is the static pressure before SWP). In some cases, this is denoted as $J_c = p/\hat{p}$, where $\hat{p}$ is pressure behind SWP. The values J_c>1 describe flow compression, while the values J_c < 1 describe flow expansion (rarefaction).

Gas-dynamic discontinuity (GDD) represents a certain idealization of an area where parameters change discontinuously, replacing the area with surfaces where gas-dynamic variables unevenly change (Uskov, Bulat & Arkhipova, 2014). GDDs in supersonic flows can be either zero-order or first order**.** Examples of zero-order GDDs include compression wave, shock wave, and sliding surface, wherein gas-dynamic flow parameters (pressure, total pressure, velocity) have discontinuities. First-order GDDs are also known as weak discontinuities (discontinuous characteristics, weak tangential discontinuities). In first-order GDDs, the first-order derivatives of gas-dynamic parameters have discontinuities.

Waves are different from discontinuities because waves have finite width and fill up the area between the leading and trailing fronts where gas-dynamic variables change from the values f to $\hat{f}$. All waves and discontinuities can be divided into two large groups (Bulat & Uskov, 2014a). The first group includes contact discontinuities (characterized by surface separating gases with different densities but equal pressures and flow velocities) and tangential discontinuities (characterized by sliding surface separating flows with equal pressures but different velocities). Gas does not flow through such surfaces. Therefore, these surfaces are not considered as SWPs. The second group includes normal waves and discontinuities (these should not be confused with straight). As gas does flow through normal waves and discontinuities, they are considered as SWPs.

Waves and discontinuities can interact with each other. There are three types of wave interactions (. Uskov, Bulat & Arkhipova, 2014b)

- GDDs (shock waves and contact discontinuities) crossing each other;
- isentropic Riemann waves interacting with each other;
- isentropic waves interacting with GDDs.

In addition, waves and discontinuities can interact with solid surfaces.

Contact and tangential discontinuities cannot cross each other. The process of shock wave or isentropic wave interaction with a contact or tangential discontinuity is called refraction. This process is accompanied by a wave refracting and reflecting at a contact (tangential) discontinuity. Other cases of wave interaction are called interference. Refraction of a moving shock wave at an inclined contact discontinuity is examined in this study.

Shock wave refraction

Several physical phenomena involving gas flows result in shock waves. Shock wave refraction problems attract increasing interest because of a wide range of possible practical applications, such as shock wave interaction with ocean surface and bubble media, underwater burst, and liquid combustion. Non-

uniform flow regions (such as high temperature areas, interfaces, dust clouds) in front of a shock wave produce qualitative changes in flow development. Examples of these phenomena include distortion of shock wave fronts, formation of new shock waves, high-pressure jets, and large-scale vortices, boundary layer separation; and jet accumulation (Jahn, 1956; Znamenskaya et al., 2011). Interaction of an oblique shock wave with an interface results in the development of complex unsteady shock wave configurations (Abd-El-Fattah & Henderson, 1978; Henderson, 1989; Henderson, 1991; Nouragliev et al., 2005). Shock waves moving through a medium containing gas bubbles or fluid globules result in distortion of shock wave fronts, shock wave accumulation, and multiple vortices.

Extant research provided a theoretical analysis of the formed shock wave configurations using shock polars (Samtaney & Zabusky, 1993). Boundaries of areas with expansion wave refraction modes and areas with the refraction of a reflected shock wave under the changing obliquity angle of a contact discontinuity were determined. Previous research also discussed vorticity generation, vortex structure evolution, and mesh convergence (Samtaney & Pullin, 1996). Studies also provided an exact solution to the problem of plane shock wave refraction at a contact discontinuity (regular case) (Samtaney, 2003; Wheatley, Pullin & Samtaney, 2005). They also discussed the suppression of the Richtmyer–Meshkov instability when a magnetic field is imposed. Exact solutions to the problem were provided for both one-dimensional and two-dimensional cases of regular shock wave refraction at a contact discontinuity.

Various shock wave refraction modes using experimental and numerical methods were examined (Zeng & Takayama, 1996). Numerical calculations were made on the basis of a TVD scheme of first-order accuracy and an approximate solution to the Riemann problem. The data obtained corresponded significantly well to the results of measurements and theoretical analysis. The only exception to this included high Mach numbers of an incident shock wave.

Two-dimensional calculations based on the Godunov-type scheme of second-order accuracy were described (Yang, 1992). Discontinuity of density was aligned at 75 degrees to the horizontal, with the Mach shock wave number of 1.2. An MUSCL scheme was used to calculate flow structure at different angles of discontinuity obliquity (Delmont, Keppens & van der Holst, 2009). Various finite difference schemes were also used in the calculations (Pember & Anderson, 2001).

A numerical study of the Richtmyer–Meshkov instability during the interaction of a strong shock wave with a linear or sinusoidal discontinuity of density was conducted (Samtaney & Meiron, 1997). Research also provided a visualization of GDD using various approaches (Samtaney & Zabusky, 2000). The refraction of a shock wave when it interacts with a near wall layer of heated gas was examined (Banuti, Grabe & Hannemann, 2011). Studies also discussed a wide range of issues associated with the interaction of shock waves with contact discontinuities and the formation of the Richtmyer–Meshkov instability (Brouillette, 2002).

The refraction of a spherical shock wave at an air–water interface was investigated (Dutta et al., 2004). The data computed were compared according to the shock-capturing scheme using the level-set method. This provides means for identifying a contact discontinuity and examining its evolution. Previous studies

discussed the application of discontinuity identification schemes with respect to the refraction of shock waves at interfaces (Liu, Khoo & Yeo, 2001) The method of characteristics was used to solve the problem at mesh nodes located near an interface. The developed approach was applied to examine shock wave interaction with a gas bubble. The level-set method was used to determine the location of a phase interface (Osher & Fedkiw, 2003). The level-set function complied with the transfer equation, and had a zero value at an interface or values opposite in sign at the areas of different phases. This made it possible to describe changes in the position of the interface. A solution method for problems with contact boundaries was also proposed (Burago & Kukudzhanov, 2005).

This study conducts numerical simulation of plane shock wave refraction at a contact discontinuity. The discontinuity is initially linear and separates gases with different densities. A case of regular shock wave refraction, when a triple configuration of GDD was formed, was investigated. This consisted of an incident shock wave, a reflected shock wave, and a transmitted shock wave. Numerical calculation data processed in the form of shadow patterns, schlieren images, and interferograms were compared with optical flow visualization data.

Flow structure

Various refraction modes emerge at the moment of shock wave incidence on a contact discontinuity positioned at a certain angle to the horizontal and separating gases with different densities. These are characterized by a refracted wave front and the formation of either an expansion wave or a reflected wave. A number of these configurations were discussed in a previous study based on the data obtained from a physical experiment (Jahn, 1956).

As a result of the interaction of the incident shock wave (I) with the contact discontinuity (C), the transmitted wave (T) and the reflected wave (R) are formed as shown in Fig. 1. These are either shock waves or expansion waves, depending on the intensity of the incident shock wave and density drop at the contact discontinuity.

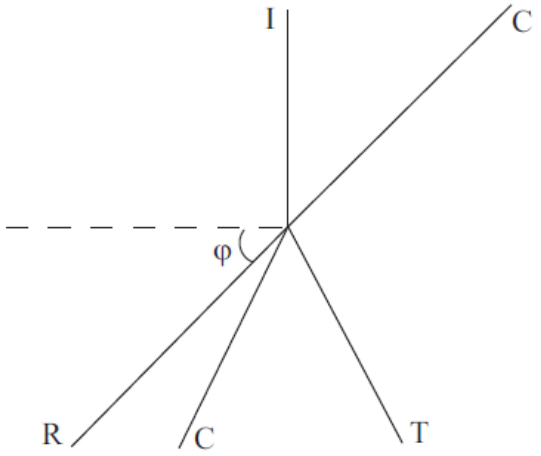

Figure 1. Shock wave refraction at a contact discontinuity

The velocity of a transmitted shock wave depends on the ratio of densities at a contact discontinuity $\sigma = \rho 2/\rho 1$. Hence, the velocity of a transmitted shock wave is either higher (slow–fast refraction, S/F) or lower (fast–slow refraction, F/S) than the velocity of an incident shock wave, depending on the ratio of surfaces (Abd-El-Fattah & Henderson, 1978; Henderson, Colella & Puckett, 1991). Velocity qualifies as the acoustic impedance of media. Word order determines the direction of wave propagation. In the slow–fast (S/F, $\sigma > 1$) case, the reflected wave is an expansion wave, while in the fast–slow (F/S, $\sigma < 1$) case, it is a shock wave. Each group (S/F and F/S) can be divided into a number of additional configurations depending on the intensity of the incident shock wave (Nouragliev, 2005). Previous researches observed 8 different refraction modes in the S/F case and 4 different refraction modes in the F/S case by changing the experimental conditions (Abd-El-Fattah & Henderson, 1978). The conditions for the existence of each mode as well as the conditions for the transition from one mode to another were also examined. The stability of the configurations was examined (Fang, Wang & Yuan, 2011).

With respect to certain parameters, a transition takes place from regular refraction (when three waves converge at a point) to non-regular refraction (when a Mach stem is formed). Extant research provides a detailed description and analysis of various modes of shock wave refraction at a contact discontinuity (Henderson, 1989; Nouragliev et al., 2005).

Computational domain and boundary conditions

The interaction of a plane shock wave moving from left to right and having a Mach number of M with a contact discontinuity oriented at the α angle to the direction of the flow is considered. The contact discontinuity separates gases with densities ρ_1 (to the left of the discontinuity) and ρ_2 (to the right of the discontinuity).

Calculations were made in the area $[0, 1] \times [0, 5]$ on an unstructured mesh containing about 10^6 nodes, with the nodes accumulated near interface. Fig. 2 shows a computational domain. In the calculations, the shock wave Mach number was assumed to be M = 2, whereas the contact discontinuity obliquity to the x-axis was $\alpha = 45°$. The contact discontinuity separated two gases with the ratio of densities $\sigma = 3$. Computational gas with the adiabatic exponent $\gamma = 1.667$ was used in the calculations. The calculations extended up to the time point $t = 0.72$ (in this time interval, a sound wave in an undisturbed gas ran across the width of a shock tube).

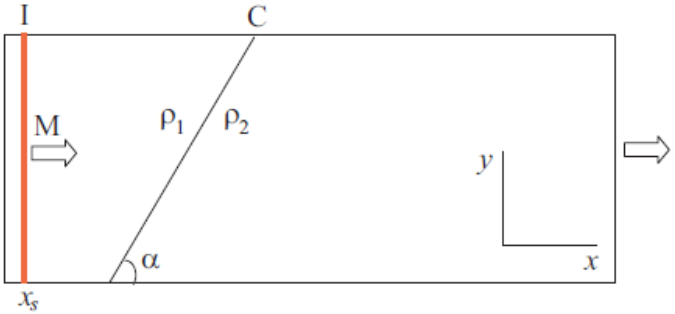

Figure 2. Computational domain

At the initial time moment, gases separated by a contact discontinuity were considered in a rest, and the shock wave front was located at xs = 0.1 (near the left boundary of the computational domain). The Rankine–Hugoniot relations were applied to the shock wave front. Non-reflecting boundary conditions were applied to the inlet and outlet boundaries of the computational domain. At the bottom boundary, symmetry conditions were applied (solid boundary).

The numerical method

The numerical model was constructed on the basis of the solution of the unsteady Euler equations for inviscid compressible gas (Volkov, 2008).

The Euler equations were discretized by the finite volume method and an explicit WENO scheme of third-order accuracy on an unstructured mesh. Previous studies provide examples of the application of WENO schemes in the simulation of supersonic flows of inviscid compressible gas on unstructured meshes (Bulat & Volkov, 2015a; Bulat & Volkov, 2015b). Convective flows were calculated independently for each direction using HLLC (Harten–Lax–van Leer–Contact) Riemann solver. Time integration was performed using a third-order Runge–Kutta method. A perfect gas equation of state with a constant ratio of specific heat capacities was used.

Discontinuity identification

The process of gas-dynamic discontinuity identification (i.e., identification of their type and position) involves considerable time and does not lack in subjectivity. A method to accelerate the process and increase its accuracy was proposed (Vorozhtsov, 1990). This involved calculating the density gradient and its orientation in the center of each mesh cell. Points with a density gradient above the average across the area were considered as points of discontinuity. GDD were classified by examining the nearest points for discrete analogs of the conditions observed at strong discontinuities. Eventually, each point belonged to a certain type of discontinuity, namely shock wave (normal or oblique), tangential discontinuity, contact discontinuity, or compression wave (Vorozhtsov, 1990).

Numerical differentiation causes noise interference in the resulting image. The order of accuracy of a finite difference scheme is decreased to the first-order near the discontinuity. This is usually required to preserve the monotonicity of the finite difference scheme. However, this also causes interference (Volkov, 2008). A smoothing operation was performed to eliminate the noise interference (Schalkoff, 1988).

Contact discontinuity identification involves the application of the level-set method. The level-set function complies with the transfer equation, and it has a zero value at an interface or values opposite in sign at the areas of different phases. This makes it possible to describe changes in the position of the interface. The condition at the contact discontinuity $\zeta(t) = 0$ makes it possible to track its position in time (on the left and right side of the discontinuity. it is assumed that $\zeta = \pm 1$).

Results and Discussions

In the calculations, the obliquity angle of a contact discontinuity to the horizontal is assumed to be $\alpha = 45°$. With the given problem parameters, a regular refraction mode was implemented, and a reflected shock wave was formed R. Samtaney, 2003. A refraction mode wherein the reflected discontinuity was an expansion wave was examined P. Delmont, R. Keppens & B. van der Holst, 2009. The case when $\alpha = 90°$ corresponded to a one-dimensional solution to the problem of shock wave interaction with a contact discontinuity.

Fig. 3 shows the density contours at the time moment $t = 0.72$. Gas density changes from 2.5 to 8.2. The density distribution shows the location of the reflected shock wave and contact discontinuity.

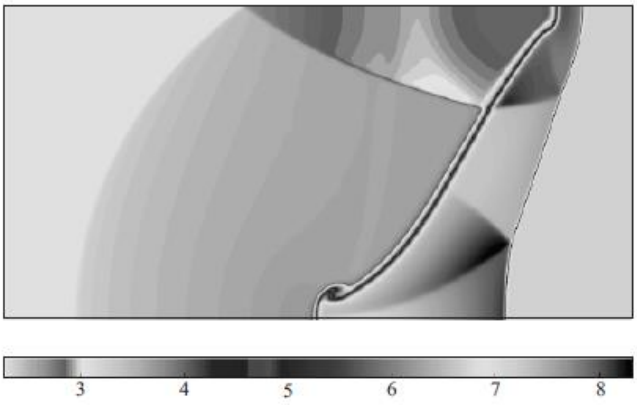

Figure 3. Contours of density

Fig. 4 shows the numerical schlieren at the time $t = 0.72$. The Sobel filter was used to discriminate discontinuities from the solution. Despite the fact that the Sobel method is less susceptible to numerical noise, in this particular problem, the use of the Roberts and Sobel operators resulted in virtually identical images (Schalkoff, 1988).

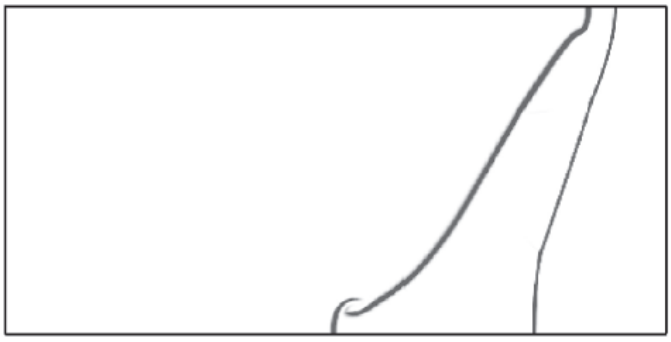

Figure 4. Numerical schlieren

Fig. 5 shows the numerical shadow pattern, and Fig. 6 shows the numerical interferogram at the time moment $t = 0.72$. Increasing the number of lines makes it possible to distinguish the flow details.

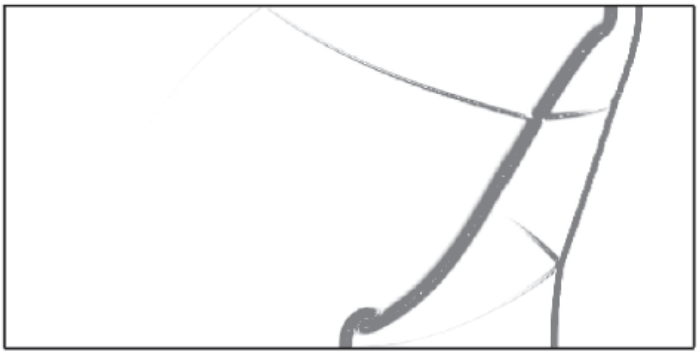

Figure 5. Numerical shadow pattern

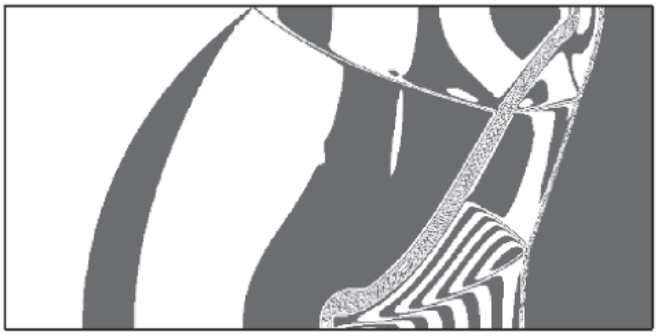

Figure 6. Numerical interferogram

Fig. 7 shows flow field visualization using different variables (pressure Laplacian, velocity divergence, entropy Laplacian). The images shown in the fragments a and b are rather similar. Conversely, using the entropy Laplacian in flow visualization (fragment c) results in a loss (invisibility) of weak gas-dynamic discontinuities.

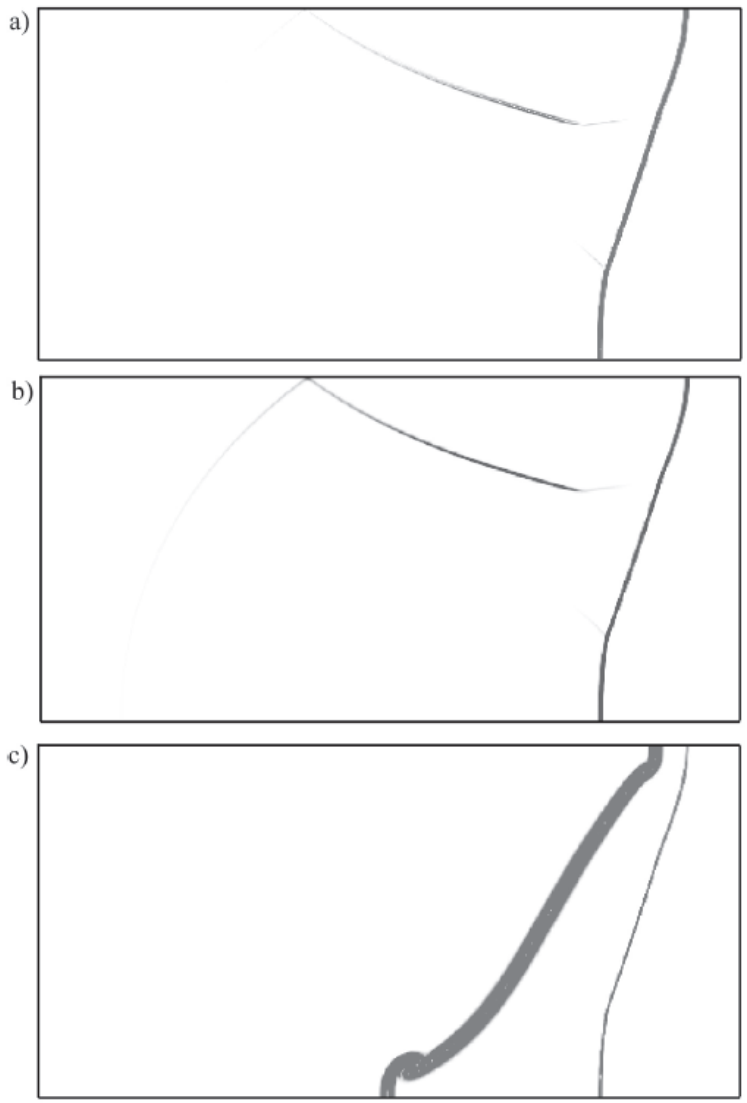

Figure 7. Flow visualization using pressure Laplacian (*a*), velocity divergence (*b*), entropy Laplacian (*c*)

Fig. 8 shows shock wave structures. The lines 1, 3, 5, 6, and 7 correspond to shock waves, while the lines 2, 4, and 8 correspond to contact discontinuities. The points T1 and T2 are triple points, where two shock waves and a contact discontinuity cross.

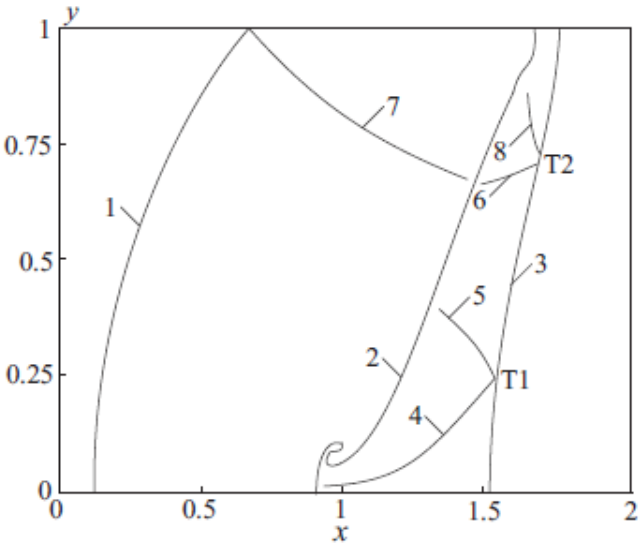

Figure 8. Shock wave structure formed as a result of shock wave interaction with a contact discontinuity

Fig. 9 shows contact discontinuity front positions determined using the density Laplacian ($\Delta\rho = 0$) and the level-set method (just a part of the computational domain is shown). Using various approaches, a significant difference in the form of determined contact discontinuity occurred only at the area of the maximum curvature. The shock wave front position depends on the approach applied for discontinuity identification. This dependence is significantly lower than that of a contact discontinuity.

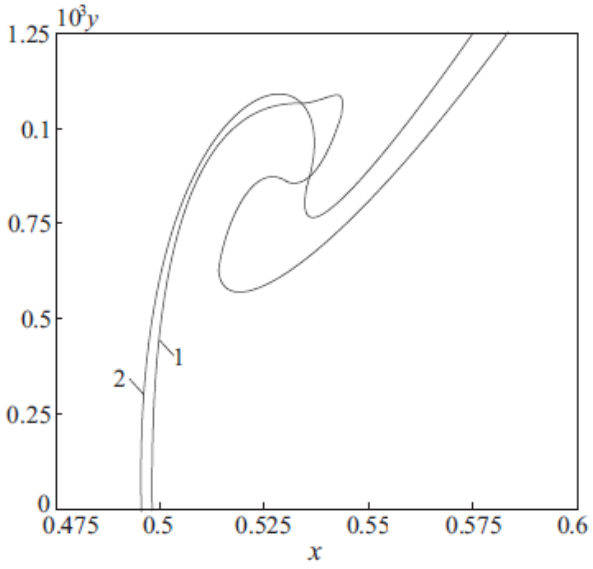

Figure 9. Contact discontinuity front positions determined using the density Laplacian (line 1) and the level-set method (line 2)

Conclusion

The interaction of a shock wave with an interface separating two gases produces a rich variety of flow phenomena even in the simplest configurations. Numerical simulation of plane shock wave interaction with an inclined contact discontinuity separating gases with different densities was performed. Results of the numerical visualization of shock wave flow patterns were compared with the data obtained from optical observations (including shadow patterns, schlieren images, and interferograms). Digital image processing methods were used to identify GDDs. The form of a contact discontinuity determined using the level-set method was compared with that obtained using a density Laplacian.

The code developed could be used to investigate wave pattern in more complex cases including transition from slow-fast to fast-slow refraction. The experimental results show that after reflection from the top wall, the contact discontinuity becomes unstable due to Kelvin–Helmholtz instability, causing it to roll up and form a Richtmyer–Meshkov instability. These instabilities are subject of intensive research and will be considered in future works. The turbulent regime posed a significant challenge, and new experimental data are required to generalize the time evolution of the interface over a wide range of initial conditions.

Acknowledgements

The research was conducted with financial support from the Ministry of Education and Science of the Russian Federation (agreement No. 14.575.21.0057), a unique identifier for Applied Scientific Research (project) RFMEFI57514X0057.

Disclosure statement

No potential conflict of interest was reported by the authors.

Notes on contributors

Pavel V. Bulat - Head of International Laboratory of Mechanics and Energy Systems, National Research University of Information Technologies, Mechanics and Optics University ITMO, Saint Petersburg, Russian Federation.

Konstantin N. Volkov - Department of Mechanical and Automotive Engineering, Senior lecturer, Kingston University, London, United Kingdom.

References

Abd-El-Fattah, A.M. & Henderson, L.F. (1978). Shock waves at a fast-slow gas interface. *Journal of Fluid Mechanics, 86*, 15–32.

Banuti, D.T., Grabe, M. & Hannemann, K. (2011). Steady shock refraction in hypersonic ramp flow. *AIAA Paper,* 2011-2215.

Brouillette, M. (2002). The Richtmyer–Meshkov instability. *Annual Review of Fluid Mechanicsm 34,* 445–468.

Bulat, P.V. & Uskov, V.N. (2014). Shock and detonation wave in terms of view of the theory of interaction gasdynamic discontinuities. *Life Science Journal, 11(8),* 307–310.

Bulat, P.V. & Volkov, K.N. (2015a). Simulation of supersonic flow in a channel with a step on nonstructured meshes with the use of the WENO scheme. *Journal of Engineering Physics and Thermophysics, 88(4),* 848–855.

Bulat, P.V. & Volkov, K.N. (2015b). Using WENO schemes for simulation of reflected shock wave with a boundary level. *Journal of Engineering Physics and Thermophysics, 88(5),* 1163–1170.

Burago, N.G. & Kukudzhanov, V.N. (2005). A review of contact algorithms. *The Institute for Problems in Mechanics of RAS, 1,* 45–87.

Delmont, P., Keppens, R. & van der Holst, B. (2009). An exact Riemann solver based solution for regular shock refraction. *Journal of Fluid Mechanics, 627*, 33–53.

Dutta, S., Glimm, J., Grove, J.W., Sharp, D.H. & Zhang, Y. (2004). Error comparison in tracked and untracked spherical simulations. *Computers and Mathematics with Applications, 48(10-11),* 1733–1747.

Fang, B., Wang, Y.G. & Yuan, H. (2011). Reflection and refraction of shocks on an interface with a reflected rarefaction wave. *Journal of Mathematical Physics, 52,* 073702.

Henderson, L.F. (1989). On the refraction of shock waves. *Journal of Fluid Mechanics, 198,* 365–386 (1989).

Henderson, L.F., Colella, P. & Puckett, E.G. (1991). On the refraction of shock waves at a slow-fast gas interface. *Journal of Fluid Mechanics, 224,* 1–27.

Jahn, R.G. (1956). The refraction of shock waves at a gaseous interface, *Journal of Fluid Mechanics, 1*, 457–489.

Liu, T.C., Khoo, B.C. & Yeo, K.S. (2001). The simulation of compressible multi-medium flow. I. A new methodology with test applications to 1D gas–gas and gas–water cases. *Computers and Fluids, 30(3),* 291–314.

Nouragliev, R.R., Sushchikh, S.Y., Dinh, T.N. & Theofanous, T.G. (2005). Shock wave refraction patterns at interfaces. *International Journal of Multiphase Flow, 31(9),* 969–995.

Osher, S.J. & Fedkiw, R.P. (2003). *Level set method and dynamic implicit surfaces*, New York: Springer, 352 p.

Pember, R.B. & Anderson, R.W. (2001). Comparison of direct Eulerian Godunov and Lagrange plus remap, artificial viscosity schemes. *AIAA Paper* 2001-2644, 255-267.

Samtaney, R. (2003). Suppression of the Richtmyer–Meshkov instability in the presence of a magnetic field. *Physics of Fluids, 15,* 53–56.

Samtaney, R. & Meiron, D.I. (1997). Hypervelocity Richtmyer–Meshkov instability. *Physics of Fluids, 9(6),* 1783–1803.

Samtaney, R. & Pullin, D.I. (1996). On initial-value and self-similar solutions of the compressible Euler equations. *Physics of Fluids, 8(10),* 2650–2655.

Samtaney, R. & Zabusky, N.J. (1993). On shock polar analysis and analytical expressions for vorticity deposition in shock-accelerated density stratified interfaces. *Physics of Fluids, 5(6),* 285–1287.

Samtaney, R. & Zabusky, N. (2000). Visualization, extraction and quantification of discontinuities in compressible flows. *Techniques and Examples*, 317-344.

Schalkoff, R.J. (1988). *Digital image processing and computer vision*. New York: John Wiley & Sons, 377 p.

Uskov, V.N., Bulat, P.V. & Arkhipova L.P. (2014a) Gas-dynamic discontinuity conception. *Research Journal of Applied Sciences, Engineering and Technology, 8(22),* 2255–2259 (2014).

Uskov, V.N., Bulat, P.V. & Arkhipova, L.P. (2014b) Classification of gas-dynamic discontinuities and their interference problems," *Research Journal of Applied Sciences, Engineering and Technology, 8(22),* 2248–2254.

Volkov, K.N. (2008). Unstructured-grid finite-volume discretization of the Navier-Stokes equations based on high-resolution difference schemes. *Computational Mathematics and Mathematical Physics, 48(7),* 1181-1202.

Vorozhtsov, E.V. (1990). On the classification of discontinuities by the pattern recognition methods. *Computers and Fluids, 18(1),* 35-74.

Wheatley, V., Pullin, D.I. & Samtaney, R. (2005). Regular shock refraction at an oblique planar density interface in magnetohydrodynamics, *Journal of Fluid Mechanics, 522***,** 179–214.

Yang, X., Chern, I., Zabusky, N.J., Samtaney, R. & Hawley, J.F. (1992). Vorticity generation and evolution in shock-accelerated density-stratified interfaces. *Physics of Fluids, 4(7),* 1531–1540.

Zeng, S. & Takayama, K. (1996). On the refraction of shock wave over a slow-fast gas interface. *Acta Astronautica, 38(11),* 829–838.

Znamenskaya, I.A., Ivanov, I.E., Koroteyeva, E.Yu. & Orlov, D.M. (2011). Gas-dynamic phenomena during shock wave interaction with the cooling plasma of impulse surface discharge. *Reports of the Russian Academy of Sciences, 439(5),* 609–612.